

# Measuring picosecond excited-state lifetimes at synchrotron sources

Bertrand Fournier\* and Philip Coppens\*

Chemistry Department, University at Buffalo, State University of New York, Buffalo, NY 14260-3000, USA. E-mail: betrandf@buffalo.edu, coppens@buffalo.edu

A new analysis method for the short excited-state lifetime measurement of photosensitive species in crystals is described. Based on photocrystallographic techniques, this method is an alternative to spectroscopic methods and is also valid for non-luminescent excited species. Two different approaches are described depending on the magnitude of the lifetime  $\tau$ . For very short lifetimes below the width of the synchrotron pulse, an estimated  $\tau$  can be obtained from the occurrence of the maximal system response as a function of the pump–probe delay time  $\Delta t$ . More precise estimates for both short and longer lifetimes can be achieved by a refinement of a model of the response as a function of the pump–probe delay time. The method also offers the possibility of the structure determination of excited species with lifetimes in the 40–100 ps range.

**Keywords:** excited-state lifetimes; photosensitive species; pump–probe delay time.

## 1. Introduction

Time-resolved photocrystallography allows the collection of dynamic structural information not accessible by other methods. By means of a pump–probe technique, it involves the measurement of light-ON and light-OFF data which are subsequently analyzed to determine time-dependent structural changes following light exposure. The theoretical aspects of ultrafast time-resolved monochromatic X-ray and electron scattering of gas-phase samples have been treated in the 1990s (Ben-Nun *et al.*, 1997; Cao & Wilson, 1998). The time dependence of the X-ray response to photo-exposure of solids is treated below. To allow single-pulse diffraction it is imperative to use the polychromatic Laue technique, which makes much more efficient use of the photon flux of the source (Makal *et al.*, 2011). To eliminate the wavelength dependence of the diffraction intensities, of the detector response and of other effects, we have introduced the RATIO method for analysis of time-resolved Laue data (Coppens *et al.*, 2009).

With a judicious choice of pump–probe delays such that the laser pulse starts close to or after the start of the X-ray pulse, and thus overlaps with the latter, it is possible to improve the time-resolution below the  $\sim 100$  ps limit of the synchrotron source. Haldrup *et al.* (2011) have measured the excitation fraction as a function of time for a species with a longer 420 ns lifetime in solution. We show here that a scan of the light response as a function of the pump–probe delay can be used for the estimate of lifetimes down to  $\sim 50$  ps without knowledge of the structure of the excited species. In favorable cases it should also be possible to determine the structures of species with such short lifetimes.

## 2. Derivation of equations

### 2.1. Experimental measurements of system response

The relative intensity response to light exposure is defined by the response ratio

$$\eta_{\mathbf{h}} = \frac{I_{\mathbf{h}}^{\text{ON}} - I_{\mathbf{h}}^{\text{OFF}}}{I_{\mathbf{h}}^{\text{OFF}}} = R_{\mathbf{h}}^{\text{ON/OFF}} - 1, \quad (1)$$

with  $R_{\mathbf{h}}$  the intensity ratio for the reflection  $\mathbf{h}$ .

We consider here the case of a single pulse without cumulative pumping in which the exposed species has only two possible states: a ground state (GS) and an excited state (ES). The latter occurs when the excitation is still significant at the time of arrival of the following laser pulse, as discussed by Fullagar *et al.* (2000). Laser exposure can be interpreted as an energy transfer and therefore,  $e_{\text{laser}}$ , the instantaneous pump laser beam intensity, as an instantaneous energy or power (mW). The instantaneous laser exposure at  $t_{\text{reference}}$  excites a fraction of sample. According to first-order kinetics, this fraction  $p$  decays as an exponential function and is given by the following. For  $t \geq t_{\text{reference}}$ ,

$$p(t_{\text{reference}}, t) = p_0 e_{\text{laser}}(t_{\text{reference}}) \exp[-(t - t_{\text{reference}})/\tau], \quad (2)$$

in which  $p_0$  is the exposure fraction of excited species per laser beam energy unit at  $t_{\text{reference}}$  in units of  $\text{mJ}^{-1}$ .

At an instant  $t$ , the total fraction  $P(t)$  of excited species results from instantaneously excited species ( $t_{\text{reference}} = t$ ) but also all remains of earlier excitations ( $t_{\text{reference}} < t$ ).  $P(t)$  is obtained by integrating  $p$  as a function of  $t_{\text{reference}}$ ,

$$P(t) = \int_{t_{\text{reference}}=-\infty}^t p_0 e_{\text{laser}}(t_{\text{reference}}) \times \exp[-(t - t_{\text{reference}})/\tau] dt_{\text{reference}}. \quad (3)$$

The total fraction  $P$  is the convolution product of the instantaneous laser beam intensity  $e_{\text{laser}}$  and the instantaneous exposure response per laser beam energy unit with  $t_{\text{reference}}$  set to zero.

For any reflection  $\mathbf{h}$ , the laser-ON intensity, diffracted by the sample when exposed to the laser light at time  $t$ ,  $i_{\mathbf{h}}^{\text{ON}}(t)$ , depends on the X-ray beam intensity at that instant  $e_{\text{xray}}(t)$  and the excited molecule fraction  $P(t)$ . The instantaneous intensity  $i_{\mathbf{h}}^{\text{ON}}(t)$  depends on the nature of the excited-state species distribution in the sample (Vorontsov & Coppens, 2005).

In the case of an excited-state cluster formation (CF),

$$i_{\mathbf{h}}^{\text{ON}}(t) = e_{\text{xray}}(t) \left\{ k |\mathbf{F}_{\mathbf{h}}^{\text{ES}}|^2 P(t) + k |\mathbf{F}_{\mathbf{h}}^{\text{GS}}|^2 [1 - P(t)] \right\}. \quad (4)$$

Here  $\mathbf{F}_{\mathbf{h}}^{\text{ES}}$  and  $\mathbf{F}_{\mathbf{h}}^{\text{GS}}$  are the ES and GS structure factors, respectively, for the structure factor, and  $k$  is a factor which depends on the volume of the crystal, the optical correction factors and the experimental details.

In the case of a random distribution of the excited-state molecules (RD), which is more commonly encountered,

$$i_{\mathbf{h}}^{\text{ON}}(t) = e_{\text{xray}}(t) k \left[ |\mathbf{F}_{\mathbf{h}}^{\text{ES}}|^2 P(t) + |\mathbf{F}_{\mathbf{h}}^{\text{GS}}|^2 [1 - P(t)] \right]^2 \quad (5)$$

which can be rewritten as

$$i_{\mathbf{h}}^{\text{ON}}(t) = e_{\text{xray}}(t) k \left[ |\mathbf{F}_{\mathbf{h}}^{\text{ES}} - \mathbf{F}_{\mathbf{h}}^{\text{GS}}|^2 P(t)^2 + |\mathbf{F}_{\mathbf{h}}^{\text{GS}}|^2 + 2P(t)(\mathbf{F}_{\mathbf{h}}^{\text{ES}} - \mathbf{F}_{\mathbf{h}}^{\text{GS}}) \cdot \mathbf{F}_{\mathbf{h}}^{\text{GS}} \right]. \quad (6)$$

Assuming small values of the conversion fraction  $P(t)$ , which is typically the case in many experiments in which the integrity of the crystal is preserved, we neglect the terms in  $P(t)^2$  to give

$$i_{\mathbf{h}}^{\text{ON}}(t) \simeq e_{\text{xray}}(t) k \left[ |\mathbf{F}_{\mathbf{h}}^{\text{GS}}|^2 + 2P(t)(\mathbf{F}_{\mathbf{h}}^{\text{ES}} - \mathbf{F}_{\mathbf{h}}^{\text{GS}}) \cdot \mathbf{F}_{\mathbf{h}}^{\text{GS}} \right]. \quad (7)$$

The total intensity  $I_{\mathbf{h}}^{\text{ON}}$  (units mJ) is obtained by integration of the instantaneous intensity  $i_{\mathbf{h}}^{\text{ON}}$  over  $t$ ,

$$I_{\mathbf{h}}^{\text{ON}} = \int_{t=-\infty}^{+\infty} i_{\mathbf{h}}^{\text{ON}}(t) dt. \quad (8)$$

If we replace  $i_{\mathbf{h}}^{\text{ON}}(t)$  by equations (4) for CF or (7) for RD and combine the terms with  $P(t)$ , we obtain  $I_{\mathbf{h}}^{\text{ON}}$  as the summation of two integrals,

$$I_{\mathbf{h}}^{\text{ON}} = \int_{t=-\infty}^{+\infty} e_{\text{xray}}(t) L_{\mathbf{h}} P(t) dt + \int_{t=-\infty}^{+\infty} e_{\text{xray}}(t) k |\mathbf{F}_{\mathbf{h}}^{\text{GS}}|^2 dt, \quad (9)$$

with, in the CF case,  $L_{\mathbf{h}} = k(|\mathbf{F}_{\mathbf{h}}^{\text{ES}}|^2 - |\mathbf{F}_{\mathbf{h}}^{\text{GS}}|^2)$  and, in the RD case with small conversion percentages,  $L_{\mathbf{h}} = k\mathbf{F}_{\mathbf{h}}^{\text{GS}} \cdot (\mathbf{F}_{\mathbf{h}}^{\text{ES}} - \mathbf{F}_{\mathbf{h}}^{\text{GS}})$ .

If we assume no variation of thermal effects, the second term of equation (9) corresponds to  $I_{\mathbf{h}}^{\text{OFF}}$ , the laser-OFF intensity of the reflection  $\mathbf{h}$ . This approximation is valid for single or few-pulse experiments, which are required for the method described here. The equation can be rewritten as

$$\eta_{\mathbf{h}} = \frac{I_{\mathbf{h}}^{\text{ON}} - I_{\mathbf{h}}^{\text{OFF}}}{I_{\mathbf{h}}^{\text{OFF}}} = H_{\mathbf{h}} \int_{t=-\infty}^{+\infty} e_{\text{xray}}(t) P(t) dt, \quad (10)$$

with  $H_{\mathbf{h}}$  a characteristic factor of  $\mathbf{h}$  defined as  $H_{\mathbf{h}} = L_{\mathbf{h}}/I_{\mathbf{h}}^{\text{OFF}}$ .

We note that the factor  $H_{\mathbf{h}}$  can be positive or negative depending on the values of  $\mathbf{F}_{\mathbf{h}}^{\text{ES}}$  and  $\mathbf{F}_{\mathbf{h}}^{\text{GS}}$  and is different for the CF and RD cases.

Substituting the expression for  $P(t)$  [equation (3)],  $\eta_{\mathbf{h}}$  becomes

$$\eta_{\mathbf{h}} = H_{\mathbf{h}} \int_{t=-\infty}^{+\infty} e_{\text{xray}}(t) \left\{ \int_{t_{\text{reference}}=-\infty}^t e_{\text{laser}}(t_{\text{reference}}) \times \exp[-(t - t_{\text{reference}})/\tau] dt_{\text{reference}} \right\} dt. \quad (11)$$

By interchanging integrals,  $\eta_{\mathbf{h}}$  can be rewritten as

$$\eta_{\mathbf{h}} = H_{\mathbf{h}} \tau \left\{ \int_{x=0}^{+\infty} \frac{\exp(-x/\tau)}{\tau} \left[ \int_{t=-\infty}^{+\infty} e_{\text{xray}}(t) e_{\text{laser}}(t - x) dt \right] dx \right\}. \quad (12)$$

The term between the square brackets is the cross-correlation of the pump and probe pulses. This equation is similar to that obtained by Cerullo *et al.* (2007) for the pump-induced variation of the probe energy in time-resolved absorption spectroscopy. If the instantaneous laser and X-ray pulse intensities  $e_{\text{laser}}$  and  $e_{\text{xray}}$  are modeled with time-dependent Gaussian functions with respective maxima  $e_{\text{laser}}^{\text{max}}$  and  $e_{\text{xray}}^{\text{max}}$  at times  $t_{\text{laser}}$  and  $t_{\text{xray}}$ , and  $\sigma_{\text{laser}}$  and  $\sigma_{\text{xray}}$  the Gaussian functions' standard deviations,  $\eta_{\mathbf{h}}$  becomes

$$\eta_{\mathbf{h}} = K_{\mathbf{h}} \tau \left[ \int_{x=0}^{+\infty} \frac{\exp(-x/\tau)}{\tau} \left( \frac{\exp\{-(x - \delta t)^2/2\sigma_{\text{M}}^2\}}{(2\pi)^{1/2}\sigma_{\text{M}}} \right) dx \right], \quad (13)$$

where  $\delta t = t_{\text{xray}} - t_{\text{laser}}$ , the pump-probe delay time, and  $\sigma_{\text{M}}^2 = \sigma_{\text{xray}}^2 + \sigma_{\text{laser}}^2$  are the parameters of the Gaussian cross-correlation function of the pump and probe pulses.  $K_{\mathbf{h}}$  equals  $p_0 e_{\text{xray}}^{\text{max}} e_{\text{laser}}^{\text{max}} H_{\mathbf{h}}$ . Thus  $\delta t$  is negative when the X-ray maximum precedes that of the laser pulse and *vice versa*.

The factor between square brackets can be interpreted as the convolution product of a normalized exponential decay function ( $\tau$ ;  $t_{\text{reference}} = 0$ ) and a Gaussian function ( $\mu = 0$ ;  $\sigma = \sigma_{\text{M}}$ ). Such a convolution product is known as an exponentially modified Gaussian function, used in chromatography for asymmetric peak fitting (Lan & Jorgenson, 2001), in theoretical biology for cell proliferation and differentiation curve fitting (Golubev, 2010) and by Gawelda *et al.* (2007) in picosecond X-ray absorption spectroscopy of solutions.

## 2.2. Infinitely sharp laser pulse approximation of the $\eta_{\mathbf{h}}$ model

The beam pulse lengths can be defined by their half-maximum intensity time windows (FWHM), labelled  $\Delta t$ , during which  $e(t) \geq e^{\text{max}}/2$ . The  $\sigma$  value is related to the FWHM by  $\sigma = \Delta t/2.355$ .

We obtain, for the ratio of width  $\Delta t$  of the two functions,

$$(\Delta t_{\text{xray}} / \Delta t_{\text{laser}})^2 = \sigma_{\text{xray}}^2 / \sigma_{\text{laser}}^2. \quad (14)$$

A  $\Delta t$  ratio larger than  $\sim 3.2$  corresponds to a  $\sigma^2$  ratio of  $\sim 10.0$ . For larger ratios,  $\sigma_{\text{M}}$  can be approximated by  $\sigma_{\text{xray}}$ , which is equivalent to modeling the laser beam pulse profile with a  $\delta$  function.

### 2.3. Exponential decay limit of the $\eta_{\text{h}}$ model

When the ES lifetime  $\tau$  significantly exceeds the laser and X-ray beam widths the limiting case is reached in which the  $\eta_{\text{h}}$  function in equation (12) approaches an exponential decay function as shown in the following.

$\eta_{\text{h}}$  can be rewritten as

$$\eta_{\text{h}} = \frac{K_{\text{h}}}{\pi^{1/2}} \left[ \int_{y = \frac{1}{\sqrt{2}} \left( \frac{\sigma_{\text{M}}}{\tau} - \frac{\delta t}{\sigma_{\text{M}}} \right)}^{+\infty} \exp(-y^2) dy \right] \exp \left[ \frac{-\delta t}{\tau} \left( 1 - \frac{\sigma_{\text{M}}^2}{2\tau\delta t} \right) \right]. \quad (15)$$

In the case that  $\sigma_{\text{M}} = (\sigma_{\text{laser}}^2 + \sigma_{\text{xray}}^2)^{1/2} \ll \delta t$  and  $\ll \tau$ , the integral limits become  $+\infty$  and  $-\infty$ , and

$$\eta_{\text{h}} \longrightarrow K_{\text{h}} \exp(-\delta t / \tau). \quad (16)$$

## 3. Dependence of the $\eta_{\text{h}}$ response profile on the time parameters

### 3.1. Normalized $\eta_{\text{h}}$ function, $\hat{\eta}_{\text{h}}$

The  $\eta_{\text{h}}$  profile depends on four time parameters:  $\sigma_{\text{laser}}$ ,  $\sigma_{\text{xray}}$ ,  $\tau$  and  $\delta t$ . As in equation (15), all variables are in ratios of parameters; multiplying each by a positive factor does not change the  $\eta_{\text{h}}$  profiles. Thus, the time parameters can be converted to be dimensionless values by division by  $\sigma_{\text{M}} = (\sigma_{\text{laser}}^2 + \sigma_{\text{xray}}^2)^{1/2}$ . This way all  $\eta_{\text{h}}$  results are valid independent of the absolute time scale,

$$\eta_{\text{h}}(\sigma_{\text{laser}}, \sigma_{\text{xray}}, \tau, \delta t) = \eta_{\text{h}} \left( \frac{\sigma_{\text{laser}}}{\sigma_{\text{M}}}, \frac{\sigma_{\text{xray}}}{\sigma_{\text{M}}}, \frac{\tau}{\sigma_{\text{M}}}, \frac{\delta t}{\sigma_{\text{M}}} \right). \quad (17)$$

Similarly, we introduce a relative lifetime  $\tau^{\text{relative}}$  and a relative delay time  $\delta t^{\text{relative}}$  defined as

$$\tau^{\text{relative}} = \tau / \sigma_{\text{M}} \quad \text{and} \quad \delta t^{\text{relative}} = \delta t / \sigma_{\text{M}}. \quad (18)$$

With typical experimental values for the beam pulse and laser windows  $\Delta_{\text{xray}}$  and  $\Delta_{\text{laser}}$ , such as  $\Delta t_{\text{laser}} = 30$  ps and  $\Delta t_{\text{xray}} = 100$  ps, we get  $\sigma_{\text{laser}} = 12.7$  ps and  $\sigma_{\text{xray}} = 42.5$  ps, which leads to  $\sigma_{\text{M}} = 43.3$  ps. According to (17),  $\eta_{\text{h}}$  becomes a function of the relative lifetime  $\tau^{\text{relative}}$  and delay time  $\delta t^{\text{relative}}$  with  $\sigma_{\text{xray}}^{\text{relative}} = 0.982$  and  $\sigma_{\text{laser}}^{\text{relative}} = 0.293$ .  $K_{\text{h}}$  is specific for each reflection  $\text{h}$  and can be positive or negative. In the following we normalize  $\eta_{\text{h}}$  by dividing by  $K_{\text{h}}$ . This means that the normalized  $\eta_{\text{h}}$ , referred to as  $\hat{\eta}_{\text{h}}$ , is always positive.

### 3.2. Plotting the $\hat{\eta}_{\text{h}}$ function

The expression of  $\hat{\eta}_{\text{h}}$  (13) does not have an analytical solution. However, it can be evaluated by using an approximation of the Gaussian error function, erf,

$$\hat{\eta}_{\text{h}} = \frac{1}{2} \left\{ 1 - \operatorname{erf} \left[ \frac{1}{2^{1/2}} \left( \frac{\sigma_{\text{M}}}{\tau} - \frac{\delta t}{\sigma_{\text{M}}} \right) \right] \right\} \exp \left[ \frac{-\delta t}{\tau} \left( 1 - \frac{\sigma_{\text{M}}^2}{2\tau\delta t} \right) \right]. \quad (19)$$

Several approximations of erf are given by Abramowitz & Stegun (1972). The approximation used in this work, which has been coded in *Python*, has a maximum error of  $1.5 \times 10^{-7}$  and is described in Appendix A.

Figs. 1(a) and 1(b) show  $\hat{\eta}_{\text{h}}$  for  $\tau^{\text{relative}}$  and  $\delta t^{\text{relative}}$  intervals of  $[0; 5\sigma_{\text{M}}]$  and  $[-2.5\sigma_{\text{M}}; 5\sigma_{\text{M}}]$  and illustrate the increase of the  $\hat{\eta}_{\text{h}}$  maximum intensity with  $\tau^{\text{relative}}$  and the  $\tau$  dependence of  $\hat{\eta}_{\text{h}}$  profile skewness as a function of  $\delta t^{\text{relative}}$ , respectively. These  $\hat{\eta}_{\text{h}}$  profiles are observed for very short positive and negative delay times when the pump and probe pulses overlap (Fig. 2a).

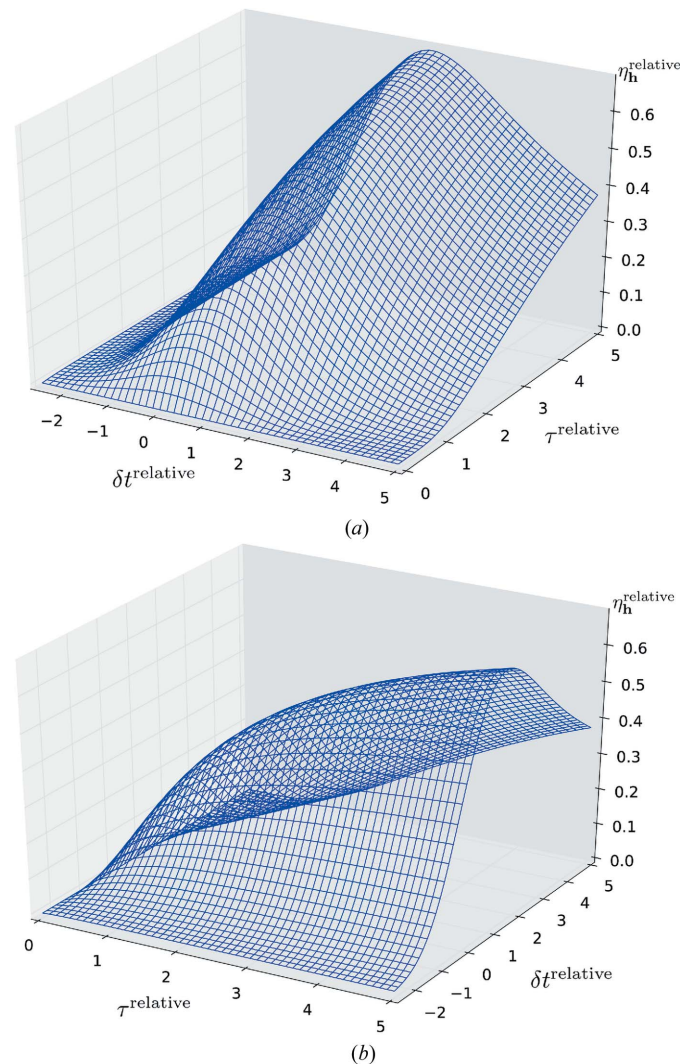


**Figure 1**

Three-dimensional plot of  $\hat{\eta}_{\text{h}}$  as a function of the relative delay time  $\delta t^{\text{relative}} = \delta t / \sigma_{\text{M}}$  and the relative lifetime  $\tau^{\text{relative}} = \tau / \sigma_{\text{M}}$ .

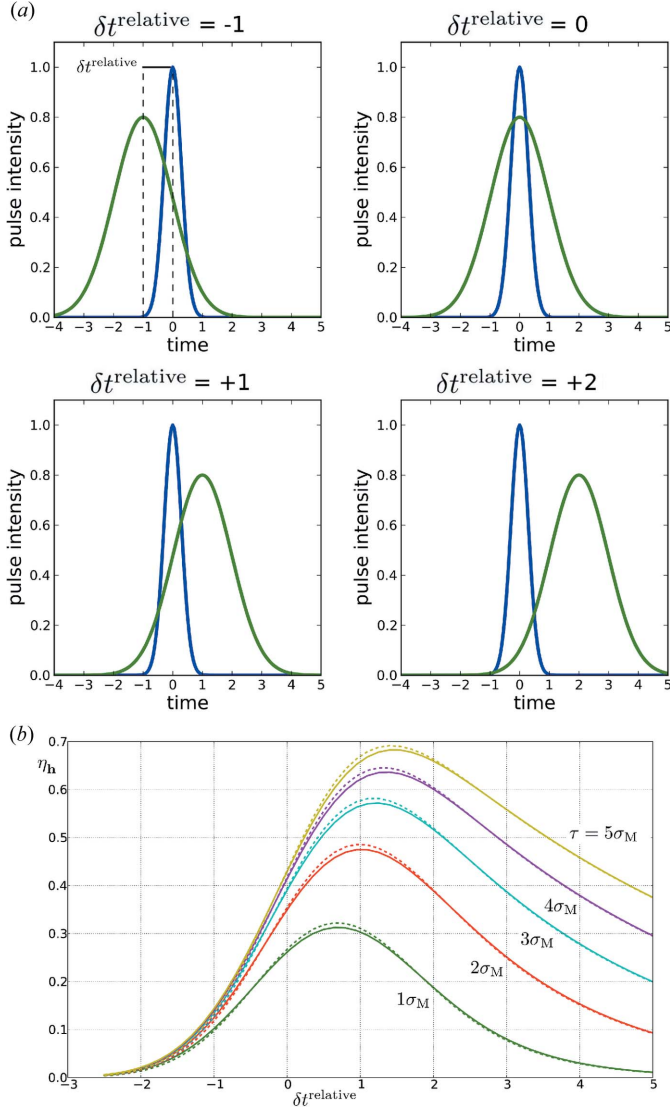


**Figure 2**  
Plots of pump-probe signals for different relative delay times  $\delta t^{\text{relative}} = \delta t / \sigma_M$  (a) and of  $\hat{\eta}_h$  as a function of  $\delta t^{\text{relative}}$  for different relative lifetimes  $\tau^{\text{relative}} = \tau / \sigma_M$  (b). In (a) the grey curves (green online) represent the laser pump pulse and the black curves (blue online) the X-ray probe pulse. In (b) the full curves represent the original  $\hat{\eta}_h$  model, and the dashed ones the approximated  $\sigma_M \simeq \sigma_{\text{xray}}$  model. The parameter  $\sigma_M = (\sigma_{\text{laser}}^2 + \sigma_{\text{xray}}^2)^{1/2}$  is  $\sim 40$  ps in our experiments. The parameter  $\delta t$  is the delay time between laser pump and X-ray pump pulse maxima.

Fig. 2(b) shows that the profile asymmetry becomes more significant as  $\tau^{\text{relative}}$  increases.

The  $\hat{\eta}_h$  values for the approximation  $\sigma_M \simeq \sigma_{\text{xray}}$  are also plotted in Fig. 2(b). The model profiles differ somewhat near their maxima. However, in both cases the maximal intensity is reached at almost the same time point  $\delta t_{\text{max}}^{\text{relative}}$  even for large  $\tau^{\text{relative}}$ .

#### 4. Methods for estimating $\tau$

To assure sufficient precision of the results the estimate of the excited-state lifetimes  $\tau$  will require closely spaced sampling of  $\delta t$  for each of the frames collected and repeated measure-

ments. As single pulse measurements are very rapid, this is entirely feasible.

Depending on the relative lifetime  $\tau^{\text{relative}} (= \tau / \sigma_M)$ , two different strategies can be used. From a mathematical point of view the  $\eta_h$  model is valid for any reflection. Nevertheless, in practice, reflections  $h$  for which absolute  $|\eta_h / \sigma_{\eta_h}|$  values are large should be selected in order to optimize the precision of  $\tau$ .

#### 4.1. Quick estimation of $\tau$ based on the position of the maximum

For each reflection used, a  $\tau^{\text{relative}}$  estimate can be deduced from the position of the  $\hat{\eta}_h$  maximum.

The derivative of  $\hat{\eta}_h$  [equation (13)] as a function of  $\delta t^{\text{relative}}$  can be expressed by interchanging the derivation and integration operators as

$$\frac{d\hat{\eta}_h}{d\delta t^{\text{relative}}}(\delta t^{\text{relative}}) = -\frac{1}{\tau^{\text{relative}}} \hat{\eta}_h(\delta t^{\text{relative}}) + \frac{1}{(2\pi)^{1/2}} \exp\left(-\frac{\delta t^{\text{relative}2}}{2}\right). \quad (20)$$

When  $\delta t^{\text{relative}} = \delta t_{\text{max}}^{\text{relative}}$ ,  $d\hat{\eta}_h(\delta t_{\text{max}}^{\text{relative}}) / d\delta t^{\text{relative}} = 0$  and at this point the  $\hat{\eta}_h(\delta t_{\text{max}}^{\text{relative}})$  value becomes

$$\hat{\eta}_h(\delta t_{\text{max}}^{\text{relative}}) = \tau^{\text{relative}} \frac{1}{(2\pi)^{1/2}} \exp\left(\frac{-\delta t_{\text{max}}^{\text{relative}2}}{2}\right). \quad (21)$$

Knowing  $\delta t_{\text{max}}$ ,  $\tau$  can be refined to satisfy equation (21) (Fig. 3). We introduce the function  $f$ , which relates  $\delta t_{\text{max}}^{\text{relative}}$  to  $\tau^{\text{relative}}$ . This function cannot be evaluated analytically, but can be approximated as  $\tilde{f}$  as described in Appendix B. Its standard deviation can be obtained from the distribution of the  $\tau^{\text{relative}}$  estimates from the individual reflections.

The relative uncertainty in  $\tau^{\text{relative}}$ ,  $\sigma_{\tau^{\text{relative}}} / \tau^{\text{relative}}$ , is related to the relative uncertainty in  $\delta t_{\text{max}}^{\text{relative}}$ ,  $\sigma_{\delta t_{\text{max}}^{\text{relative}}} / \delta t_{\text{max}}^{\text{relative}}$ , as explained in Appendix B.

Fig. 4 shows that the ratio of the relative uncertainties in  $\tau^{\text{relative}}$  and  $\delta t_{\text{max}}^{\text{relative}}$ , ratio $_{\sigma}$ , plotted as a function of  $\delta t_{\text{max}}^{\text{relative}}$ ,

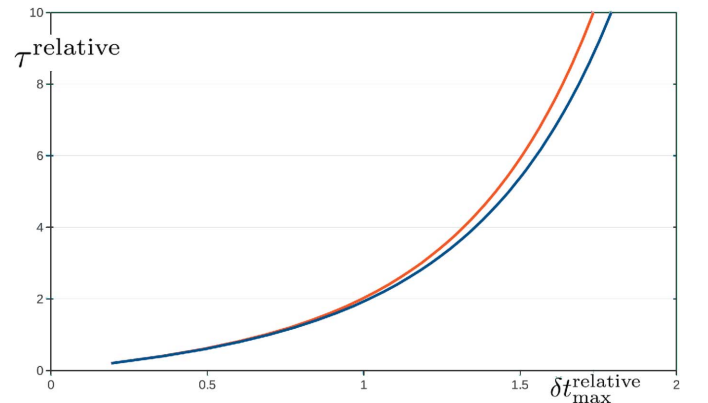


**Figure 3**  
Plot of the relative lifetime  $\tau^{\text{relative}} = \tau / \sigma_M$  as a function of the relative delay time  $\delta t_{\text{max}}^{\text{relative}} = \delta t_{\text{max}} / \sigma_M$ , with  $\delta t_{\text{max}}$  the instant at which  $\hat{\eta}_h$  is maximal. The black line (blue online) corresponds to the original  $\hat{\eta}_h$  model, and the grey line (orange online) to the approximated  $\sigma_M \simeq \sigma_{\text{xray}}$  model.

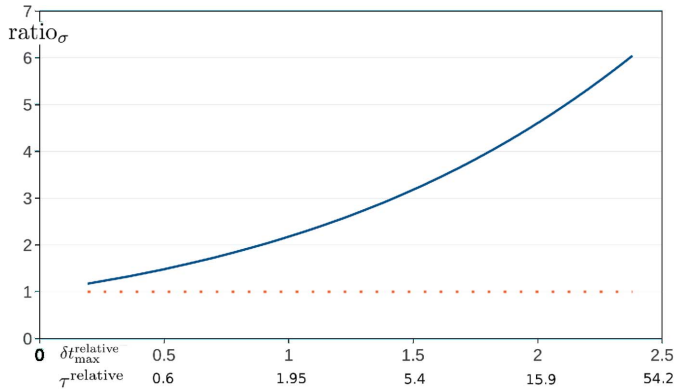


**Figure 4**  
Plot of  $\text{ratio}_\sigma$ , the ratio of the relative uncertainties in  $\tau^{\text{relative}} = \tau/\sigma_M$  and  $\delta t_{\text{max}}^{\text{relative}} = \delta t_{\text{max}}/\sigma_M$ , with  $\delta t_{\text{max}}$  the instant at which  $\hat{\eta}_h$  is maximal.  $\text{ratio}_\sigma$  is drawn as a function of  $\delta t_{\text{max}}^{\text{relative}}$ . The corresponding  $\tau^{\text{relative}}$  values are also given on the  $x$  axis. The orange dotted line corresponds to the constant function  $\text{ratio}_\sigma = 1$ .

increases with  $\delta t_{\text{max}}^{\text{relative}}$  and  $\text{ratio}_\sigma(\delta t_{\text{max}}^{\text{relative}}) \geq 1$  or  $\sigma_{\tau^{\text{relative}}}/\tau^{\text{relative}} \geq \sigma_{\delta t_{\text{max}}^{\text{relative}}}/\delta t_{\text{max}}^{\text{relative}}$ . It follows from the  $\text{ratio}_\sigma$  profile that the uncertainties are different for short- and long-lifetime  $\tau$ . Thus the uncertainties in  $\tau^{\text{relative}}$  increase with  $\delta t_{\text{max}}^{\text{relative}}$ . A more precise estimate can be obtained by refinement of a model of the system response as a function of  $\delta t^{\text{relative}}$  as described in the following section.

#### 4.2. Least-squares fitting of the $\eta_h$ function

A more precise procedure is to perform a global least-squares (LS) fitting of the  $\eta_h$  model against the full set of  $\eta_h$  values collected for  $N_h$  different reflections with different  $\delta t$ , with, as variables,  $\tau$  plus  $N_h$  multiplicative factors  $K_h$  (one per reflection). The minimized LS error function  $\varepsilon$  will be

$$\varepsilon = \sum_h w_h \left\{ \sum_{i=1}^{N_{\delta t}} [\eta_h^{\text{measured}}(\delta t_i) - \eta_h^{\text{model}}(\delta t_i)]^2 \right\}. \quad (22)$$

If intensities are collected with a significant redundancy, a weighting scheme can be introduced using  $\sigma_{\eta_h^{\text{mean}}}$  to give  $w_h = 1/\sigma_{\eta_h^{\text{mean}}}^2$ .

Finally, if the preliminary plots of  $\eta_h$  values as a function of  $\delta t$  reveal a monotonic decreasing of  $\eta_h$ , the LS fitting can be based on the simple exponential decay of  $\eta_h$ .

## 5. Conclusions and perspectives

The measurement of an excited-state lifetime using photocrystallographic techniques is an alternative to spectroscopic methods for subnanosecond lifetimes, provided sufficient precision is achieved by repeated measurement if necessary. Furthermore, it allows the measurement of lifetimes of non-luminescent excited states, which is of importance when the emission is quenched by non-radiative processes. In all cases it is necessary to closely sample  $\delta t$ .

## APPENDIX A

### Approximation of erf

The approximation of erf used in this work is defined as

$$\begin{aligned} \text{erf}(x) &= \frac{2}{\pi^{1/2}} \int_{y=0}^x \exp(-y^2) dy \\ &\simeq \text{sign}(x) \left[ 1 - (a_1 t + a_2 t^2 + a_3 t^3 \right. \\ &\quad \left. + a_4 t^4 + a_5 t^5) \exp(-x^2) \right] \end{aligned} \quad (23)$$

where

$$t = \frac{1}{1 + p|x|}$$

with  $p = 0.3275911$ ,  $a_1 = 0.254829592$ ,  $a_2 = -0.284496736$ ,  $a_3 = 1.421413741$ ,  $a_4 = -1.453152027$ ,  $a_5 = 1.061405429$ .

## APPENDIX B

### Approximation of $\tau$ as a function of $\delta t_{\text{max}}$

In §4.1 we introduce a quick estimation method of  $\tau^{\text{relative}}$  based on the  $\delta t_{\text{max}}^{\text{relative}}$  estimate. The function  $f$  which gives, for each  $\delta t_{\text{max}}^{\text{relative}}$ , the corresponding  $\tau^{\text{relative}}$  is unknown. However, some characteristics of  $f$  can be obtained.

#### B1. Asymptotic behavior of $f$

The following relation between  $\tau^{\text{relative}}$  and  $\delta t_{\text{max}}^{\text{relative}}$  can be deduced from equations (15) and (21),

$$\left[ \int_{y=U}^{+\infty} \exp(-y^2) dy \right] \exp(U^2) = \tau^{\text{relative}}/2^{1/2}, \quad (24)$$

with  $U = (1/2^{1/2})(1/\tau^{\text{relative}} - \delta t_{\text{max}}^{\text{relative}})$ .

The asymptotic behaviors of  $f$  at  $+\infty$  and at  $0^+$  (the positive side of 0) can be deduced from this expression (see supplementary material<sup>1</sup>).

$$\tau^{\text{relative}} \underset{+\infty}{\sim} (2\pi)^{1/2} \exp\left(\delta t_{\text{max}}^{\text{relative}2}/2\right) \quad (25)$$

and

$$\tau^{\text{relative}} \underset{0^+}{\sim} \delta t_{\text{max}}^{\text{relative}}. \quad (26)$$

#### B2. Approximation function $\tilde{f}$

Taking into account the asymptotic behaviors of  $f$ , an approximation can be defined as

$$\begin{aligned} \tilde{f}(\delta t_{\text{max}}^{\text{relative}}) &= (2\pi)^{1/2} \left[ \exp\left(\frac{\delta t_{\text{max}}^{\text{relative}2}}{2}\right) \right. \\ &\quad \left. + \frac{\delta t_{\text{max}}^{\text{relative}} \exp(-\delta t_{\text{max}}^{\text{relative}})}{(2\pi)^{1/2}} - 1 \right]. \end{aligned} \quad (27)$$

$f$  and  $\tilde{f}$  share the same asymptotic behaviors. The absolute error remains reasonable, even for large  $\tau^{\text{relative}}$ . For instance,

<sup>1</sup> Supplementary data for this paper are available from the IUCr electronic archives (Reference: VV5035). Services for accessing these data are described at the back of the journal.

for  $\delta t_{\max}^{\text{relative}} = 2.65$ ,  $f(2.65) = 80$ , while  $\tilde{f}(2.65) \simeq 80.7$ . For all  $\delta t_{\max}^{\text{relative}} \in ]0; +\infty[$ , the relative error of  $\tau^{\text{relative}}$  is smaller than 4%.

### B3. Ratio of relative uncertainties $\text{ratio}_\sigma$

According to the propagation of errors, the approximate uncertainty in  $\delta t_{\max}^{\text{relative}}$  is related to the uncertainty in  $\tau^{\text{relative}}$  as follows, where  $f'$  is the derivative of  $f$ ,

$$\sigma_{\tau^{\text{relative}}} = |f'(\delta t_{\max}^{\text{relative}})| \sigma_{\delta t_{\max}^{\text{relative}}}, \quad (28)$$

which gives, for the relative uncertainties,

$$\frac{\sigma_{\tau^{\text{relative}}}}{\tau^{\text{relative}}} = \frac{|f'(\delta t_{\max}^{\text{relative}})| \delta t_{\max}^{\text{relative}}}{f(\delta t_{\max}^{\text{relative}})} \frac{\sigma_{\delta t_{\max}^{\text{relative}}}}{\delta t_{\max}^{\text{relative}}}. \quad (29)$$

We define the function  $\text{ratio}_\sigma$  for  $\delta t_{\max}^{\text{relative}} \in ]0, +\infty[$  as

$$\text{ratio}_\sigma(\delta t_{\max}^{\text{relative}}) = \frac{\sigma_{\tau^{\text{relative}}} / \tau^{\text{relative}}}{\sigma_{\delta t_{\max}^{\text{relative}}} / \delta t_{\max}^{\text{relative}}} = \frac{|f'(\delta t_{\max}^{\text{relative}})| \delta t_{\max}^{\text{relative}}}{f(\delta t_{\max}^{\text{relative}})}. \quad (30)$$

Support of this work by the National Science Foundation (CHE0843922) is gratefully acknowledged.

### References

- Abramowitz, M. & Stegun, I. A. (1972). *Handbook of Mathematical Functions with Formulas, Graphs, and Mathematical Tables*. New York: Dover.
- Ben-Nun, M., Cao, J. & Wilson, K. R. (1997). *J. Phys. Chem. A*, **101**, 8743–8761.
- Cao, J. & Wilson, K. R. (1998). *J. Phys. Chem. A*, **102**, 9523–9530.
- Cerullo, G., Manzoni, C., Luer, L. & Polli, D. (2007). *Photochem. Photobiol. Sci.* **6**, 135–144.
- Coppens, P., Pitak, M., Gembicky, M., Messerschmidt, M., Scheins, S., Benedict, J., Adachi, S., Sato, T., Nozawa, S., Ichiyangi, K., Chollet, M. & Koshihara, S. (2009). *J. Synchrotron Rad.* **16**, 226–230.
- Fullagar, W. K., Wu, G., Kim, C., Ribaud, L., Sagerman, G. & Coppens, P. (2000). *J. Synchrotron Rad.* **7**, 229–235.
- Gawelda, W., Pham, V.-T., Benfatto, M., Zaushitsyn, Y., Kaiser, M., Grolimund, D., Johnson, S. L., Abela, R., Hauser, A., Bressler, C. & Chergui, M. (2007). *Phys. Rev. Lett.* **98**, 057401.
- Golubev, A. (2010). *J. Theor. Biol.* **262**, 257–266.
- Haldrup, K., Harlang, T., Christensen, M., Dohn, A., van Driel, T. B., Kjær, K. S., Harrit, N., Vibenholt, J., Guerin, L., Wulff, M. & Nielsen, M. M. (2011). *Inorg. Chem.* **50**, 9329–9336.
- Lan, K. & Jorgenson, J. W. (2001). *J. Chromatogr. A*, **915**, 1–13.
- Makal, A., Trzop, E., Sokolow, J., Kalinowski, J., Benedict, J. & Coppens, P. (2011). *Acta Cryst.* **A67**, 319–326.
- Vorontsov, I. I. & Coppens, P. (2005). *J. Synchrotron Rad.* **12**, 488–493.